THE UNIVERSITY OF MELBOURNE

Robotics Systems
MCEN90028

Robotic Systems: Assignment 1

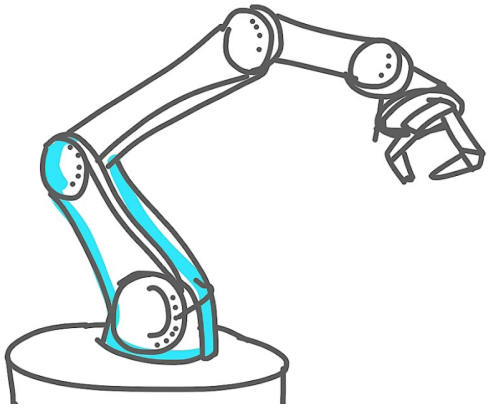

Authors:
David Pham 756598
Pamela Kong 833891
Thomas Pimenta 763237

March 31, 2021

1 Introduction

The objective of this project is to design and manufacture a robotic system that is capable of moving chess pieces along a chessboard. The moves must be legal as prescribed in the official FIDE rules of chess. The purpose of this assignment is to outline the proposed solution for this project, derive the forward and inverse kinematics of the designed robot, and to determine the necessary link lengths of the robot in order to reach the workspace as required by the chessboard used in the project.

2 Identification of Problem

The important considerations for this problem involve the size of the selected board, the necessary degrees of freedom and the mechanical components involved in the fabrication.

2.1 Components, Board and Degrees of Freedom

The provisional choice for the selected board is the Classic Games Chess board manufactured by Merchant Ambassador (Holdings) Ltd. with dimensions 360mm by 360mm. This choice was made since one of the team members owned the board and so it was easily accessible. However, should problems arise with this selection in the future, alternative boards may be considered.

Before generating a proposed solution, it was relevant to identify the necessary degrees of freedom (DoF). From a 3-dimensional Cartesian perspective, the necessary degrees of freedom would be 4: 3 DoF for the robot's movement in the x, y and z directions, as well as 1 DoF for the pinching motion of the grasping mechanism. However, this is merely the bare minimum required as there may need to be additional degrees of freedom to model the spherical coordinates of a moving robotic arm.

2.2 Proposed Solutions

The first instinct of the team was to try and generate a solution similar to a human arm. This would have 2 DoF rotations at the origin followed by a link which is equivalent to a shoulder. This would connect with a single DoF revolute joint connected to another link acting as an elbow. This in turn would have 2 DoF rotation connected to a gripper which would be the equivalent of wrists and fingers.

Another alternative but similar approach that was considered was to build an arm also with 2 DoF revolutions at the base connected to a link and a single DoF revolute joint at what can be considered the elbow. However at this point there would also be a prismatic joint allowing for a link to be extended towards the board which would be connected to a gripper. This design was considered cumbersome and inefficient as the link would have to be quite long and a prismatic joint would be slower than strategically placed revolute joints.

A final alternative approach considered was to have an external frame built above the board with runners in the x and y planes. These would allow for a gripping device to be located above the desired piece and then lowered with relatively few moving parts. Unfortunately discussion with the subject moderator revealed that such a design was not within the scope of the project.

3 Forward Kinematics

Once a design idea was selected it was necessary to analyse the forward kinematics in order to generate a transformation matrix from the task space to the end effector in the joint space. The team generated the following illustration which isolated each joint so that one degree of freedom was considered at a time. This was necessary to construct the transformation matrix as described by the Denavit-Hartenberg (D-H) convention. The chosen idea was represented in Figure 1 where Frame 0 is the inertial frame at the decided origin.

For ease of understanding the team equivocated the design to a human arm. Frames 1 and 2 are considered to be a part of the shoulder, Frame 3 is the elbow, Frames 4 and 5 pertain to the movement of the wrist and Frame 6 to the grip of the fingers. It is vital to note that Frame 5 will always be fixed in orientation from the perspective of the origin frame. This was a design choice made to minimise the potential for errors while grasping and replacing pieces, especially non-symmetric ones like the knight. Additionally it was decided that the wrist should always point vertically down to minimise the chance of releasing pieces at an angle that may

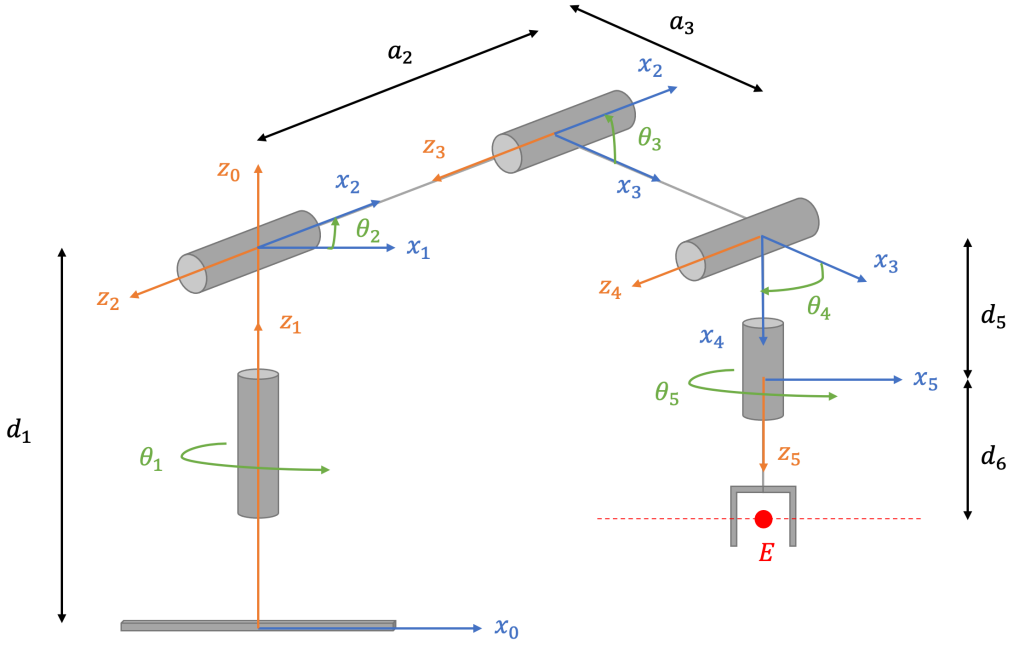

Figure 1: Physical Representation of System

cause them to topple over which would constrain the z-axis of Frame 4 to be parallel to the z-axis of the origin.

This generated the following D-H table:

i	a_{i-1}	α_{i-1}	d_i	Q_i
1	0	0	d_1	θ_1
2	0	90°	d_2	θ_2
3	a_2	0	d_3	θ_3
4	a_3	0	d_4	θ_4
5	0	90°	d_5	θ_5
6	0	0	d_6	Q_6

Table 1: D-H Table generated from design

In the above table a_2 and a_3 determine the link lengths; d_2, d_3, and d_4 represent offsets where the joints meet; d_1 represents the height that the first motor sits at above the chess board; and d_5 represents the distance from the base of the wrist to the base of the gripper and d_6 is the distance from the wrist base to point of contact for gripping. Q_6 is the motor angle variable associated with the gripper

To construct transformation matrices in between each consecutive frame it was necessary to follow the following formula:

$$ {}^{0}_{1}T = D_x(a_{i-1}).R_x(\alpha_{i-1}).D_z(d_i).R_z(\theta_i) \tag{1} $$

Where:

$$ \begin{aligned} D_x(a_{i-1}) &= \begin{bmatrix} 1 & 0 & 0 & a_{i-1} \\ 0 & 1 & 0 & 0 \\ 0 & 0 & 1 & 0 \\ 0 & 0 & 0 & 1 \end{bmatrix}; R_x(\alpha_{i-1}) = \begin{bmatrix} 1 & 0 & 0 & 0 \\ 0 & cos(\alpha_{i-1}) & -sin(\alpha_{i-1}) & 0 \\ 0 & sin(\alpha_{i-1}) & cos(\alpha_{i-1}) & 0 \\ 0 & 0 & 0 & 1 \end{bmatrix}; \\ D_z(d_i) &= \begin{bmatrix} 1 & 0 & 0 & 0 \\ 0 & 1 & 0 & 0 \\ 0 & 0 & 1 & d_i \\ 0 & 0 & 0 & 1 \end{bmatrix}; R_z(\theta_i) = \begin{bmatrix} cos(\theta_i) & -sin(\theta_i) & 0 & 0 \\ sin(\theta_i) & cos(\theta_i) & 0 & 0 \\ 0 & 0 & 1 & 0 \\ 0 & 0 & 0 & 1 \end{bmatrix} \end{aligned} \tag{2} $$

The concatenation gives the generic transform between each frame of:

$$ {}^{i-1}_{i}T = \begin{bmatrix} cos(\theta_i) & -sin(\theta_i) & 0 & a_{i-1} \\ cos(\alpha_{i-1}).sin(\theta_i) & cos(\alpha_{i-1}).cos(\theta_i) & -sin(\alpha_{i-1}) & -d_i.sin(\alpha_{i-1}) \\ sin(\alpha_{i-1}).sin(\theta_i) & sin(\alpha_{i-1}).cos(\theta_i) & cos(\alpha_{i-1}) & d_i.cos(\alpha_{i-1}). \\ 0 & 0 & 0 & 1 \end{bmatrix} \tag{3} $$

With the knowledge of the constraints on Frames 5 and 6 it was possible to calculate the position of the end effector by simply transforming between Frames 0 and 4, from the origin to the base of the wrist and then subtracting d_5 and d_6 in the z-plane such that the vertical distance to the point of contact was accounted for.

The transformation was obtained via the following process:

$$ {}^{0}_{4}T = {}^{0}_{1}T.{}^{1}_{2}T.{}^{2}_{3}T.{}^{3}_{4}T \tag{4} $$

The transformation matrix can be broken down into constituent parts to extract the relevant position equations.

$$ {}^{0}_{4}T = \begin{bmatrix} \mathbf{R} & \mathbf{T} \\ \mathbf{0} & 1 \end{bmatrix} \tag{5} $$

Where:

$$ \mathbf{0} = [0 \quad 0 \quad 0] \tag{6} $$

$$ \mathbf{R} = \begin{bmatrix} R_{11} & R_{12} & R_{13} \\ R_{21} & R_{22} & R_{23} \\ R_{31} & R_{32} & R_{33} \end{bmatrix} \tag{7} $$

$$ R_{11} = cos(\theta_1)\cdot(-cos(\theta_4)\cdot(sin(\theta_2)\cdot sin(\theta_3) - cos(\theta_2)cos(\theta_3)) - sin(\theta_4)\cdot(cos(\theta_2)\cdot sin(\theta_3) + cos(\theta_3)\cdot sin(\theta_2))) \tag{8} $$

$$ R_{12} = cos(\theta_1)\cdot(cos(\theta_4)\cdot(cos(\theta_2)\cdot sin(\theta_3) + cos(\theta_3)\cdot sin(\theta_2)) - sin(\theta_4)\cdot(sin(\theta_2)\cdot sin(\theta_3) - cos(\theta_2)\cdot cos(\theta_3))) \tag{9} $$

$$ R_{13} = sin(\theta_1) \tag{10} $$

$$ R_{21} = sin(\theta_1)\cdot(cos(\theta_4)\cdot(sin(\theta_2)\cdot sin(\theta_3) - cos(\theta_2)\cdot cos(\theta_3)) + sin(\theta_4)\cdot(cos(\theta_2)\cdot sin(\theta_3) + cos(\theta_3)\cdot sin(\theta_2))) \tag{11} $$

$$ R_{22} = sin(\theta_1)\cdot(sin(\theta_4)\cdot(sin(\theta_2)\cdot sin(\theta_3) - cos(\theta_2)\cdot cos(\theta_3)) - cos(\theta_4)\cdot(cos(\theta_2)\cdot sin(\theta_3) + cos(\theta_3)\cdot sin(\theta_2))) \tag{12} $$

$$ R_{23} = cos(\theta_1) \tag{13} $$

$$ R_{31} = cos(\theta_4)\cdot(cos(\theta_2)\cdot sin(\theta_3) + cos(\theta_3)\cdot sin(\theta_2)) + sin(\theta_4)\cdot(cos(\theta_2)\cdot cos(\theta_3) - sin(\theta_2)\cdot sin(\theta_3)) \tag{14} $$

$$ R_{32} = sin(\theta_4)\cdot(cos(\theta_2)\cdot sin(\theta_3) + cos(\theta_3)\cdot sin(\theta_2)) - cos(\theta_4)\cdot(cos(\theta_2)\cdot cos(\theta_3) - sin(\theta_2)\cdot sin(\theta_3)) \tag{15} $$

$$ R_{33} = 0 \tag{16} $$

$$ \mathbf{T} = \begin{bmatrix} x \\ y \\ z \end{bmatrix} \tag{17} $$

The equations obtained from the transformation were:

$$x = -a_3 \cdot cos(\theta_1) \cdot (sin(\theta_2) \cdot sin(\theta_3) - cos(\theta_2) \cdot cos(\theta_3)) + sin(\theta_1) \cdot (d_2 + d_3 + d_4) + a_2 \cdot cos(\theta_1) \cdot cos(\theta_2) \quad (18)$$

$$y = a_3 \cdot sin(\theta_1) \cdot (sin(\theta_2) \cdot sin(\theta_3) - cos(\theta_2) \cdot cos(\theta_3)) + cos(\theta_1) \cdot (d_2 + d_3 + d_4) - a_2 \cdot cos(\theta_2) \cdot sin(\theta_1) \quad (19)$$

$$z = d_1 + a_3 \cdot sin(\theta_2 + \theta_3) + a_2 \cdot sin(\theta_2) \quad (20)$$

This provided the equation for the position of the wrist and it was a simple matter of offsetting the z value by $d_5 + d_6$ to find the task space coordinates of the end effector.

$$z = d_1 - (d_5 + d_6) + a_3.sin(\theta_2 + \theta_3) + a_2.sin(\theta_2) \quad (21)$$

The z equation was purely in terms of θ_2 and θ_3 and the expected vertical displacements. The team found it gratifying as it made sense with the teams physical understanding of the system.

4 Determination of Link Lengths

When designing the robot for our project a key consideration is the physical geometry of the design. In order to identify appropriate link lengths for the robot simulations were made in MATLAB that would determine the reachable area of design subject to certain constraints.

These simulations would iterate through various combinations of angles and determine the task space coordinates of the end effector. The team chose to simplify the problem using the knowledge that the gripping mechanism will always be pointing down vertical to the ground. This is a design choice to minimise the chance of pieces falling when released in the desired location. With this knowledge the team could calculate the pose of the wrist component (origin of Frame 4) and factor in the height of the gripping mechanism as a constant in the z-plane.

4.1 Constraints at Joints

In order to plot the reachable workspace it was necessary to determine the constraints of each joint. From the data sheet it was known that the Serial Bus Smart Control servo SCS15 had a displacement range between 0° and 200°. This would be the maximum range but there would be further constraints possible to optimise the calculations.

θ_1 would be constrained between 0° and 90° as the robot was designed to be placed at the corner and this was the maximum angular displacement needed to cover the board area. θ_2 was constrained between 10° and 90°. The lower limit was determined in order to prevent any potential elbow up configurations and to minimise the chances of the first link knocking over any pieces near the board. θ_3 was constrained between 0° and 150°. When θ_3 is 0° the two links are fully extended and as it approaches 180° the two links fold into each other. A safety margin of 30° was deemed appropriate to factor in any geometric incompatibilities at extreme cases. Similar logic was used to set θ_4 constraints to be between 0° and 150°. As will be discussed in section 5 the value for θ_5 depends on θ_1 so will have the same constraints of 0° and 90°. Due to the nature of the chosen design outlined in Figure 1 the values for θ_2 and θ_3 have to be negative. The following table summarises the angular constraints of the joints.

Angle	Lower Bound (°)	Upper Bound (°)
1	0	90
2	10	90
3	-150	0
4	-150	0
5	0	90

Table 2: Acceptable Range of Angles

Initial sizes for links a_2 and a_3 were set at 500mm and varied in order to observe the impact on the reachable workspace and obtain a more holistic understanding of the system kinematics. Two graphs were drawn at each stage, one parallel to the y-plane demonstrating how x and z coordinates varied for a side view; and one parallel

to the z-plane to demonstrate how x and y coordinates varied for a top down view.

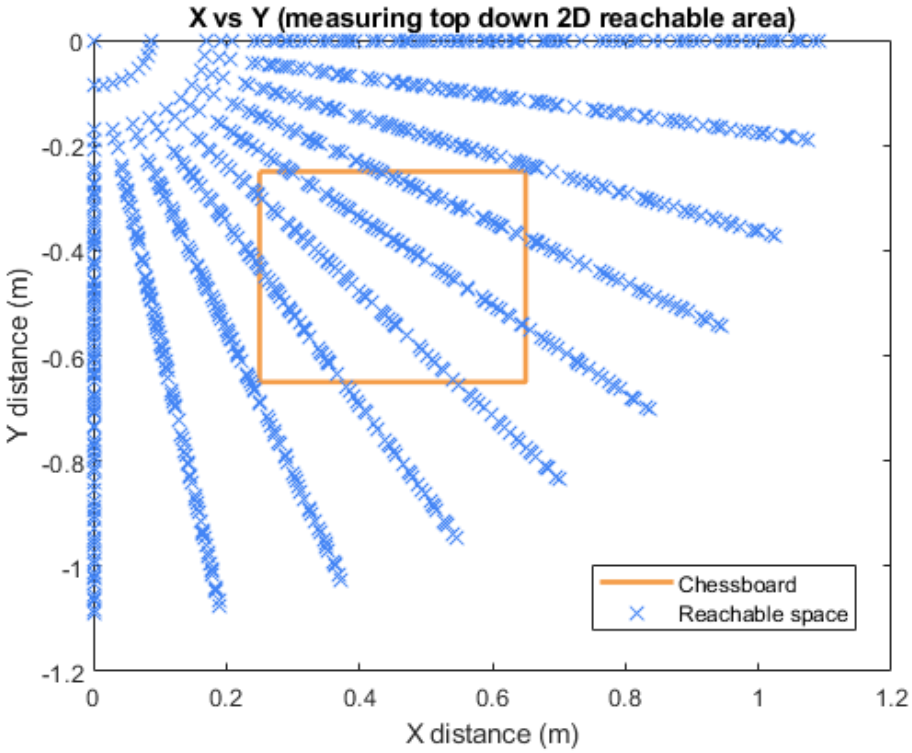

Figure 2: Top-Down View of Reachable Workspace and ChessBoard

In this graph the link lengths were $a_2 = 600$mm and $a_3 = 500$mm. Several lengths were tested but much smaller than these and there was very limited potential to reach the entire board. Any larger was not unnecessary to reach the board and would cause undue stress and excessive torque on the motors. As can be seen in Figures 2 and 3 the desired workspace is more than sufficient. The team opted for a cautious approach in allowing for broad reachable areas so as to minimise the effect of modelling errors and provide more flexibility for any unforeseen circumstances that may arise in the manufacturing stage.

The radial spokes that can be seen in Figure 2 are due to the nature of how the angles were iterated in the for loops on MATLAB. As θ_1 was on the outermost loop it would have the slowest increments which led to the pattern displayed. In Figure 3 certain values appear to be well beyond the board but as can be corroborated by observing Figure 2 these would only apply to extreme cases of θ_1 where the board would not be reached from the perspective of the y-coordinate.

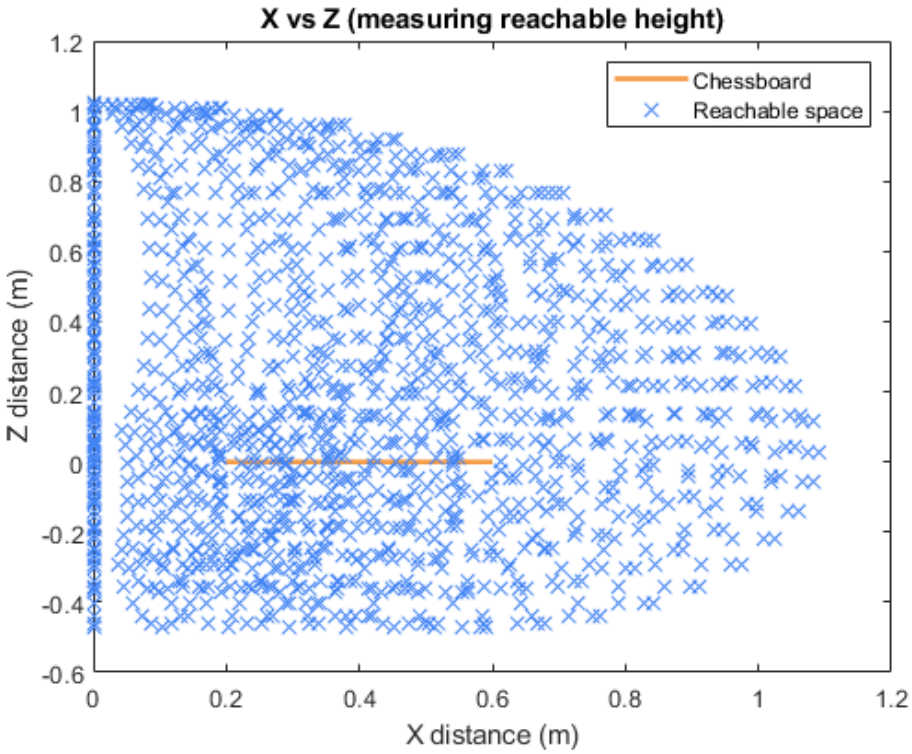

Figure 3: Side View of Reachable Workspace and ChessBoard

5 Inverse Kinematics

It was also necessary to be able to derive what the combination of angles would be necessary to reach a given set of task space coordinates. This would be used in order to locate pieces on the board and place them in their new locations. For this the team would need to implement inverse kinematics.

5.1 Geometric Analysis and Constraints

The team initially sought to find a geometric representation in order to minimise computational complexity for the problem. Using the geometric constraints described in section 3 the team could establish a relationship between certain angles. The desire to keep the wrist pointing vertically down at all times allowed for the team to draw the following quadrilateral shape:

The angles being $\theta_2, \theta_3, \theta_4$ and a fixed 90° angle between the z_5 axis and the table. Using the knowledge that the interior angles of a quadrilateral sum to 360° a relationship could be established.

$$360 = |\theta_2| + (180 - |\theta_3|) + (180 - |\theta_4|) + 90 \tag{22}$$

$$|\theta_4| = |\theta_2| - |\theta_3| + 90 \tag{23}$$

Another constraint that allowed for a relationship to be established was that between θ_1 and θ_5. The gripper orientation is desired to point in a forward orientation regardless of how θ_1 swivels about the robot arm's "shoulder". Due to the nature of the behaviour of the arm as shown in Figure 5 it was established that the relationship follows:

$$\theta_5 = \theta_1 \tag{24}$$

Although geometrically they should share a negative relationship, Frames 1 and 5 have opposite facing z-axis which ensures opposite rotations. The angle θ_1 can also be obtained geometrically. This is a very simple relationship and can be visualised in Figure 2:

$$\theta_1 = tan^{-1}(\frac{-y}{x}) \tag{25}$$

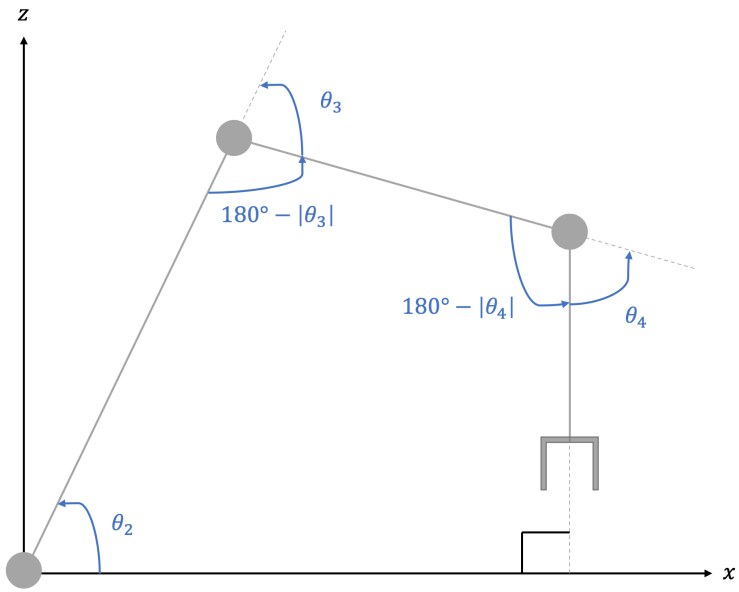

Figure 4: Quadrilateral that describes angle θ_4

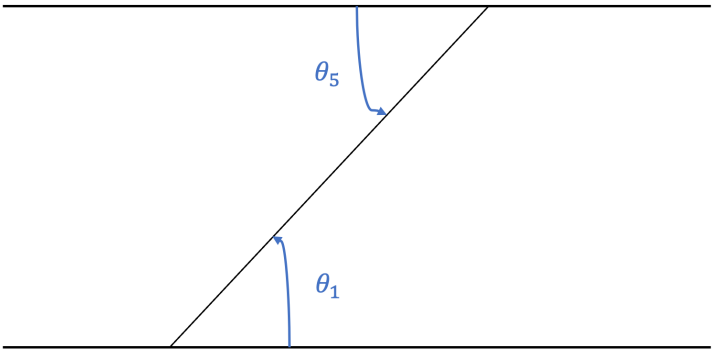

Figure 5: Relationship between θ_1 and θ_5

5.2 General Approach to Inverse Kinematics

Given the forward kinematic equations are known, the general approach is to use matrix inversion multiplication.

$$coeffs \cdot \begin{bmatrix} \theta_1 \\ \theta_2 \\ \theta_3 \end{bmatrix} = \begin{bmatrix} x \\ y \\ z \end{bmatrix} \qquad \Rightarrow \qquad \begin{bmatrix} \theta_1 \\ \theta_2 \\ \theta_3 \end{bmatrix} = Inv(coeffs) \cdot \begin{bmatrix} x \\ y \\ z \end{bmatrix}$$

The approach first collapses the systems of equations into matrix form. This requires that the theta angles can be decoupled before the coefficients are inverted and multiplied over to the Cartesian coordinates. The current issue is that this method requires linear equations and that the theta angles can be decoupled. As the equations of motion have a mix of sinusoids and multiplied elements, it is algebraically strenuous to directly decouple these.

$$x = a2 \cdot cos(\theta_1) \cdot cos(\theta_2) - a3 \cdot (cos(\theta_1) \cdot sin(\theta_2) \cdot sin(\theta_3) - cos(\theta_1) \cdot cos(\theta_2) \cdot cos(\theta_3)) \tag{26}$$

$$y = a3 \cdot (sin(\theta_1) \cdot sin(\theta_2) \cdot sin(\theta_3) - cos(\theta_2) \cdot cos(\theta_3) \cdot sin(\theta_1)) - a2 \cdot cos(\theta_2) \cdot sin(\theta_1) \tag{27}$$

$$z = d1 - d5 - d6 + a3 \cdot sin(\theta_2 + \theta_3) + a2 \cdot sin(\theta_2) \tag{28}$$

A simple and computationally concise approach is to linearise these equations, this enables both eased decoupling and linear equations to generate inverse kinematic equations. By then using Taylor's series we can approximate the kinematic behaviour around equilibria points that exist within our previously mentioned acceptable range of theta angles. Equilibria points are found where the derivative of the system is 0. As our equations describe position, the derivative equations are all cartesian velocities. The intended mode of robot arm operation is to receive a command, move and be stationary before receiving another command. Therefore between motions, the robot arm is moving from equilibria. As a result all points within our reachable workspace are valid equilibria so long as velocity was 0 before estimating and that the robot arm travels small distances.

5.3 Equations

The two chosen points of equilibria for $(\theta_1, \theta_2, \theta_3)$ include:
$S1 = (\frac{\pi}{4}, \frac{\pi}{4}, \frac{\pi}{4})$, an elbow extended position and
$S2 = (\frac{\pi}{4}, \frac{\pi}{3}, \frac{4\pi}{3})$, an elbow bent in position both common orientations for grabbing chess pieces.

$$\theta_{1,S1} = \frac{-(x+y)}{a_2} \tag{29}$$

$$\theta_{2,S1} = \frac{2^{0.5} \cdot z}{a_2} \tag{30}$$

$$\theta_{3,S1} = \frac{2^{0.5} \cdot (y-x)}{2 \cdot a_3} - \frac{z \cdot a_2 + 2^{0.5} \cdot a_3}{a_2 \cdot a_3} \tag{31}$$

$$\theta_{1,S2} = -\frac{2^{0.5} \cdot (x-y)}{a_2 + a_3} \tag{32}$$

$$\theta_{2,S2} = \frac{z}{a_2} + \frac{2^{0.5} \cdot 3^{0.5} \cdot (y-x)}{6 \cdot a_2} \tag{33}$$

$$\theta_{3,S3} = \frac{2^{0.5} \cdot z \cdot 2^{0.5}(\cdot a_2 - a_3)}{2 \cdot a_2 \cdot a_3} + \frac{2^{0.5} \cdot 3^{0.5} \cdot (x-y) \cdot (a_2 + a_3)}{6 \cdot a_2 \cdot a_3} \tag{34}$$

From the reference ground frame, θ_1 being a purely horizontal rotation will only relate to the x and y-coordinates and have no contribution to the z-component. This is reflected in our inverse kinematic equations, where both sets are purely in terms of x and y variables.

As θ_2 and θ_3 extend from θ_1 and contribute to end effector elevation, they in turn relate to all x,y and z axis.

6 Conclusion

Within this part of the project, the team identified various potential solutions and settled on what felt like an achievable and intuitive design. From this point equations were derived to obtain task space coordinates from given angular rotations using forward kinematics. These equations were then used to generate an outline of the potential reachable workspaces for given angles and parameters. Once this had been achieved inverse kinematic equations were developed so that the robot could reach a desired task space.

The team ends this stage of the project with an understanding of the kinematics of the chosen system and a clear vision for how it will interact with the chessboard. A platform has been set so that future work on relating joint velocities to end effector velocity and necessary torques to overcome the gravitational forces induced by the mass of the links.